Desalination and Water Treatment
www.deswater.com

doi: 10.5004/dwt.2021.26781

219 (2021) 96–102
April

Stability analysis of cemented paste backfill false roof in highwall mining: a case study

Qingliang Chang[a], Xikui Sun[b], Xiangjian Dong[c,*], Sihua Shao[d]

[a]*Key Laboratory of Deep Coal Resource Mining, Ministry of Education of China, School of Mines, China University of Mining & Technology, Xuzhou 221116, China*
[b]*Shandong Energy Zibo Mining Group CO., LTD., Zibo 255120, China*
[c]*Department of Civil, Environmental and Mining Engineering, The University of Western Australia, Crawley WA 6009, Australia, email: xiangjian.dong@research.uwa.edu.au*
[d]*Gansu Jingyuan Coal Industry and Electricity Power Co., Ltd., School of Mines, China University of Mining and Technology, Xuzhou 221116, China, email: shaosihuajm@163.com*

Received 15 August 2020; Accepted 23 November 2020

ABSTRACT

The highwall mining technique is widely used to extend the life of open-pit mines without disturbing the surface dwellings, while maintaining economy and productivity. In this paper, the theoretical analysis, numerical simulation and material testing methods were used to study the damage form of the false roof in Juhugeng No. 7 mine with highwall cemented paste backfill (CPB) mining of Qinghai Yanhu Group. The CPB strength effect on the false roof stability and its control are investigated in detail. The results show that the main failure mode of the false roof is breaking failure, which is mainly affected by the strength of the CPB. The simulation study found that when the strength of CPB is increased from 0.5 to 1.5 MPa, the stress of the false roof is reduced to about 1/3, and the vertical displacement is decreased from 6.8 to 4.4 mm. When the strength is changed to 3.0 MPa, the vertical displacement is further reduced to around 50%, and the vertical stress and the surrounding plastic zone are greatly dropped correspondently. It can be seen that the strength of the CPB is essential to ensure the stability of the false roof. Furthermore, the preliminary tests of the filling material show that the cement dosage, rock fineness and mass concentration have significant effect on improving the quality of CPB and guarantee the stability of false roof, it is conducive to the safe and efficient exploitation of the slicing mining with CPB.

Keywords: CPB; Highwall mining; Slicing mining; Stability of false roof; Strength of CPB

1. Introduction

The stability control of roof strata is one of the most difficult problems in coal mine operations [1–3]. Recently, the analytical solutions [4–6], numerical simulations [7–9] and experimental analyses [10,11] have extensively been conducted to investigate the mechanism of rock failure under various conditions. Lots of techniques have been developed to maintain the safety of the surrounding rock mass. Among them the backfilling technique, which offers both economic and environmental benefits, has been widely used in both the underground and open-pit mines in China. It limits the likelihood of caving and prevents roof subsidence.

Highwall mining technique is generally used in the end slope remnant coal mining of open-pit mine [12–16]. Under the thick coal seam condition, the downward slicing mining method is usually adopted. When the backfill with CPB is used in the method, the strength of the false roof formed by CPB in upper slice is the key determinant of mine safety production. Many related researches pointed out that the factors, including filling material characteristics, artificial false roof construction technique and mining operation

* Corresponding author.

design, affected the stability of the artificial false roof. Among these quantitative and qualitative influencing factors, the first two variables control the strength of the bearing layer while the mining operation design mainly affects the stress state of the bearing layer [17–19].

Furthermore, the studies on the false roof thickness and its limited span effect on the overall stability of the chain pillars in thick coal seam operation indicated that the thickness of backfilling roof should not exceed a limit value [20–25]. There exists an extreme point in the relationship of the false roof limited span and its thickness. Although the paste filling mining technology has experienced rapid development, the research on the stability of false roof with highwall paste filling mining is limited.

Juhugeng No. 7 mine false roof stability was analysed as a case study, which is located in Tianjun County of Haixi state, Qinghai province, about 5 km east-west and 1 km south-north. The recoverable reserve is 36.99 Mt with an area of 5.08 km^2. Over the years, the massive pits and waste hills have been caused by the long-term traditional open-pit mining and resulted in serious destruction to the fragile environment and regional landscape. The main coal seams of No. 7 mine are 1F and 2F coal seams with the average thickness of 9.20 and 11.46 m, respectively. The coal seam interval is about 54.32 m with average dip angle of 62°–88°. The mining process is to downward excavate an access roadway across the two main coal seams in the mining area. In the meantime, excavate the roadway by the method of unmanned downward mining with end slope shearer along the coal seam strike and fill the goaf without delay.

The CPB in upper slice can not only control the overlying strata deformation effectively but also serve as the roof when mining the lower slice. Therefore, it is necessary for safety and highly efficient coal mining to study the influence factors and control methods of the stability of backfill. Based on the highwall downward slicing mining with paste filling in Juhugeng No. 7 mine of Qinghai Yanhu Group, a mechanical model of false roof formed by CPB was set up. In order to provide technical support for the safety production of mine with paste filling slicing, the research focuses on the effect of strength on the stability of false roof and the control methods, and it is of great realistic significance to apply the paste filling in the thick coal seam slicing mining and green mining.

2. Mechanical analysis of stability of false roof

According to the mining scheme of descending slicing, the upper and lower layers of the roadway are designed to be offset by a certain distance in the horizontal direction. The main reason is that the immediate roof and floor of 1F and 2F are soft mudstone, and it is easy to produce vertical shear stress in the weak plane of the false roof. The weak plane is shown in Fig. 1. Compared with CPB, there exists more joint fissure in the coal body. In addition, the CPB has strong compactness and integrity. Therefore, the reliability of research results can be guaranteed by the design of setting coal pillars on both sides of roadway (Fig. 1).

Some scholars have applied the basic theory of elastic mechanics to study the stress state of the artificial false roof and the mechanism of the instability was obtained.

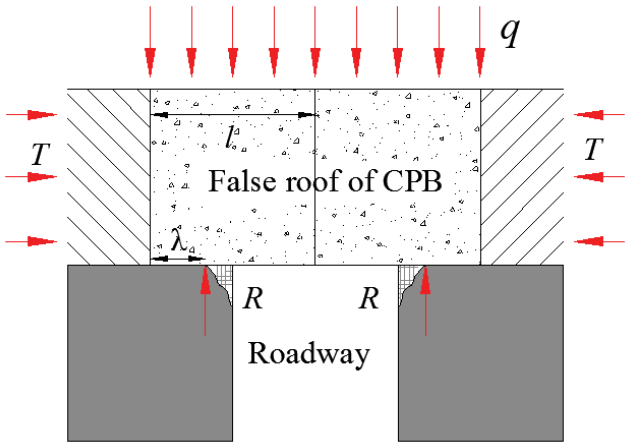

Fig. 1. Mechanical analysis model of false roof stability.

The false roof stability mechanical analysis models of thin plate model and simply supported beam model based on the "plate structure based on both sides of elastic foundation" are proposed, but there are some differences in terms of the application situations. The thin plate model is suitable for parallel layout of the upper and lower layers, while the latter applies to the case where the upper and lower stratified approaches are vertical or inclined. According to the mining design scheme of No. 7 mine, the analytical model is established based on the thin plate mechanical model as shown in Fig. 1.

2.1. Breaking failure

The false roof formed can be supported effectively by collar pillars when the plastic zone of the pillars is very small. The false roof is mainly affected by the strength of the CPB, which has the risk of cutting off or breaking while it is not prone to overall slippage or rotation instability.

2.1.1. Cutting failure

The shear force of the false roof can be written as follows:

$$R = q(l - \lambda) \tag{1}$$

where q is the uniform load on the false roof; l represents the width of mining roadway; λ is the distance of the inner edge in the plastic zone of the coal pillar to the weak plane of the false roof.

False roof remains stable when the shear stress of CPB is less than the allowable shear stress [τ]. The maximum shear stress of the false roof can be expressed as follows:

$$\tau_{max} = \frac{q(l - \lambda)k}{h} \tag{2}$$

where k is the safety factor, h is the height of the false roof.

In order to ensure the reliability of false roof and consider the most unfavorable state, τ_{max} is then calculated to be the cohesion strength (C) by letting normal stress

equals to zero (σ_c = 0). Based on the laboratory compression test results of the paste filling material, the relationship between cohesion and strength is obtained as: $C = 0.173\sigma_c - 0.1$. Therefore, the strength of backfill material follows the following equation:

$$\sigma_c = \frac{q(l-\lambda)k}{0.173h} + 0.578 \tag{3}$$

According to the composite beam theory, the overlying strata and the CPB have no force on the false roof, so the uniform load ($q = \gamma h$) can be estimated only when the weight is considered. q was calculated to be 0.0594 MPa by letting γ = 0.018 N/m^3, h = 3.3 m.

Considering the most unfavorable circumstances, the plastic zone of coal pillar reaches its maximum value (λ_{min} = 0) and k = 1.2. The designed compression strength of the CPB should be larger than 0.95 MPa (σ_c > 0.95 MPa) to avoid the occurrence of the cutting failure.

2.1.2. Tensile failure

There exists weak structural plane between the adjacent false roof above the roadway under the condition that the false roof is filled for several steps, so the stability of false roof can be analyzed based on the cantilever beam theory.

The bending moment of the false roof is expressed as follows:

$$M = \frac{q(l-\lambda)^2}{2} \tag{4}$$

The tensile stress at a point in the cross section is calculated as follows:

$$\sigma_t = \frac{My}{I_z} \tag{5}$$

where I_z and y represent the moment of inertia of the cross section and the distance between stress point and neutral axis z, respectively. Therefore, the maximum tensile stress of the false roof appears when $y = h/2$, and the moment of inertia is written as: $I_z = bh^3/12$. Substituting the parameters, the maximum tensile stress in this case is calculated as 0.146 MPa.

To ensure that no false roof tensile failure occurred, the required compressive strength of CPB was calculated to be atleast 1.17 MPa assuming that the compression strength is eight times of the tensile strength.

2.2. Rotational failure

Rotational failure refers to the state that the local position turns to plastic state and/or even further large rotation deformation due to the concentration of local compression stress. The whole structure then fails to withstand the upper strata. The mechanic model is shown in Fig. 2.

For this static state, the bending moment at point O is zero ($\Sigma M_O = 0$), we have:

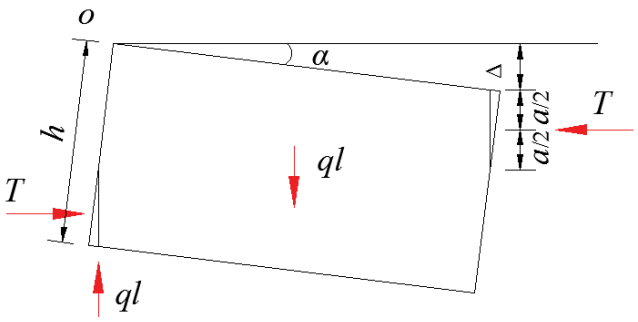

Fig. 2. Mechanical analysis of roof structure rotational failure.

$$T(h-a-\Delta) = \frac{ql^2}{2} \tag{6}$$

Assuming the occlusal point is in the plastic state into consideration, the action point of T takes $a/2$ place and Δ can be approximately taken as $l\sin\alpha$ ($\Delta = l\sin\alpha$). According to the geometrical relationship we have:

$$a = \frac{(h - l\sin\alpha)}{2} \tag{7}$$

$$T = \frac{ql^2}{h - l\sin\alpha} \tag{8}$$

The extrusion stress σ_p can be calculated as follows:

$$\sigma_p = \frac{T}{a} = \frac{2ql^2}{(h - l\sin\alpha)^2} = \frac{2qi^2}{(1 - i\sin\alpha)^2} \tag{9}$$

where $i = l/h$. We use k to represent the ratio of the extrusion strength (σ_p) to the allowable compressive strength ([σ_c]), the allowable load is derived as follows:

$$q = \frac{k(1 - i\sin\alpha)^2[\sigma_c]}{2i^2} \tag{10}$$

The final displacement of the false roof then can be calculated as follows:

$$\Delta = \left(h - \sqrt{\frac{2q}{k[\sigma_c]}}l\right) \tag{11}$$

Finally, based on the above calculation analysis, rotary distortion instability will happen when the subsidence (Δ) of the false roof reaches 2.3 m. But according to the practical experience of the CPB false roof, the maximum subsidence of the roof is about 300 mm. Obviously, the possibility of the occurrence of rotary distortion instability is very small.

3. Numerical simulation of false roof stability

The software adopted in the numerical simulation is FLAC3D (Fast Lagrangian Analysis of Continua). According to the general conditions of No. 7 mine geologic condition,

due to the large interval between coal seams, the interaction of backfill mining the two steep coal seams (1F and 2F) are relatively small. In order to avoid the repeated calculation, the numerical model only reflects the process of filling mining in the 2F coal seam. The range of the coal seam dip angle is 62°–88°. Mechanical factors such as the cumulative deformation and the vertical stress in the process of downward mining are unfavorable to the stability of the false roof, especially under the large dip angle condition. The mechanical properties of the rock mass are listed in Table 1. This simulation analyses the most unfavorable situation with a dip angle of 90°. Both the height and width of the model are set to 94 m. The distance from the upper boundary to the surface is 70 m. The model is restricted to horizontal movement and the lower boundary is fixed. The uniform hydrostatic pressure is applied on the top boundary of the model, which is calculated as 1.7 MPa. The model geometry and its boundary conditions are shown in Fig. 3.

The stability of false roof above the mining roadway was analyzed with the influence of different strength grades (0.5/1.5/3.0 MPa) of CPB. The plastic zone, displacement field and stress contour are the main characters for the stability of the false roof. As shown in Fig. 3, the coal seam was excavated with filling roadway mining method and four roadways 6-3-7-4 represent the design sequence of CPB mining. To keep the consistency with the mining site, the false roofs are divided into five strength grades. The stratum strength directly upon the roadway, No. 1, is set as 3 d age strength (the formation of the CPB has 3 d). The strength of the second stratum No. 2 is set as 10 d age strength. The strength of the No. 3, 4 and 5 strata is 17, 24 and 28 d age strength of filling material, respectively. The upmost strength of the curing time is 28 d age strength. The mechanical behavior of CPB is summarized in Table 2.

4. Experiment of the influence factors on material strength

According to the above analysis, the strength of CPB plays an important role in the stability of false roof. The preliminary test of CPB material was carried out in this section. The experimental materials include waste rock, Zhonglian P.O42.5 ordinary Portland cement, water and additive (PA Beifu agentia). The effect of cement dosage, rock fineness (the content of 0.08 mm fine particles in processing waste) and mass concentration on strength of false roof were mainly studied to reflect the adjustment and control the various factors on the stability of false roof.

5. Results and discussion

5.1. Filling material effect on the strength of the CPB

The 3-d CPB strength is the minimum age strength of the false roof based on the mining scheme. Therefore, to maintain the false roof stability, the strength of CPB after 3-d solidification must reach the required strength as previously described as 1.17 MPa. From Fig. 4, after the filling material has been fully reacted, the age strength of 3 d was significantly increased compared with that of 1 d. Fig. 4a indicates that the cement content should not be less than 150 kg/m^3. It can be seen that when the mass concentration changes 1% of the compression strength of the CPB changes in the range of 10%–25%. The effect of concentration

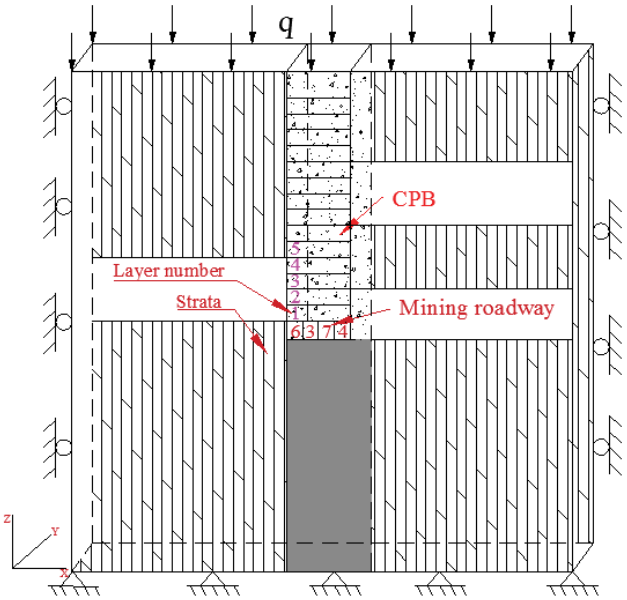

Fig. 3. Geometric model for simulating the stability of false roof.

Table 1
Rock mechanical parameters for the simulation

Strata No.	Name	Lithology	Bulk modulus K/GPa	Shear modulus G/GPa	Internal friction angle ϕ/°	Cohesion C/MPa	Tensile strength σt/MPa	Density kg/m^3
1	Immediate roof	Coarse sandstone	19	23,917	32.08	11.89	0.16	2,567
2	False roof	Mudstone	6.7	4,167	38.00	2.44	0.01	2,493
3	Coking coal	2F	0.6	288	28.00	5.40	0.07	1,500
4	False bottom	Mudstone	6.7	4,167	38.00	2.44	0.01	2,493
5	Immediate floor	Fine-sandstone	22	14,007	32.83	8.40	0.07	2,599
6	Immediate roof1	Medium sandstone	52	4,850	42.00	1.80	0.11	2,650

Table 2
Mechanical parameters of CPB in simulation

Strength grade/ age 28 d	Bulk modulus/ GPa	Shear modulus/ GPa	Internal friction angle/°	Cohesion/ MPa	Tensile strength/ MPa
Grade 0.5 MPa	0.049	0.021	35.678	0.203	0.074
Grade 1.5 MPa	0.087	0.038	35.678	0.360	0.188
Grade 3.0 MPa	0.155	0.068	35.678	0.640	0.390

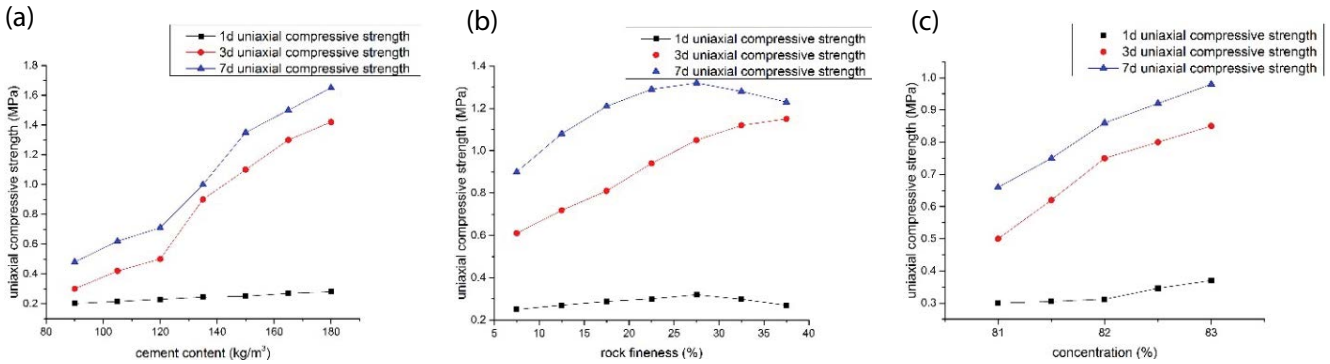

Fig. 4. Relationship between the strength of false roof and filling material (a) cement content, (b) rock fineness, and (c) mass concentration.

on the strength of false roof is obvious. In prerequisite of meeting flow properties of filling slurry, the concentration would better be improved to reduce the amount of cement and avoid excessive waste processing. Finally, low-cost paste filling mining can be achieved under the condition of satisfying the requirement of false roof stability.

5.2. Effect of CPB strength on the stress and displacement of false roof

The simulation results were mainly aimed at roadway No. 7. As shown in Fig. 5, when the strengths of the CPB were 0.5 and 1.5 MPa, the vertical stress at the top of the roadway No. 1 was 0.021 and 0.008 MPa, respectively. When the strength increased to 3 MPa, the false roof was almost free of vertical stress, which is also in agreement with the theoretical calculation process of the uniform load that ignores the vertical stress of overlying strata. It can be seen in Fig. 6 that the average vertical displacement of CPB was 6.8, 4.4 and 2.6 mm and the corresponding strength of CPB was 0.5, 1.5 and 3 MPa, respectively. It shows that the displacement decreases with the increase of the CPB strength.

5.3. Effect of CPB strength on the plastic zone of false roof

As shown in Fig. 7, when the strength of the CPB was 0.5 MPa, the plastic zone around the false roof widely distributed and the stability was greatly affected; when the strength reached 1.5 MPa, the plastic zone appeared partially in the upper and lower boundary region of the false roof and the stability was good. When the strength of the CPB was increased to 3 MPa, there is almost no plastic zone and the stability of roof reached its optimal.

6. Conclusions

The safety production of highwall mining is highly affected by the upper strata stability. The stability of false roof, formed by CPB in downward slicing method, and its control in Juhugeng No. 7 mine are investigated with various methods. The main findings are as follows:

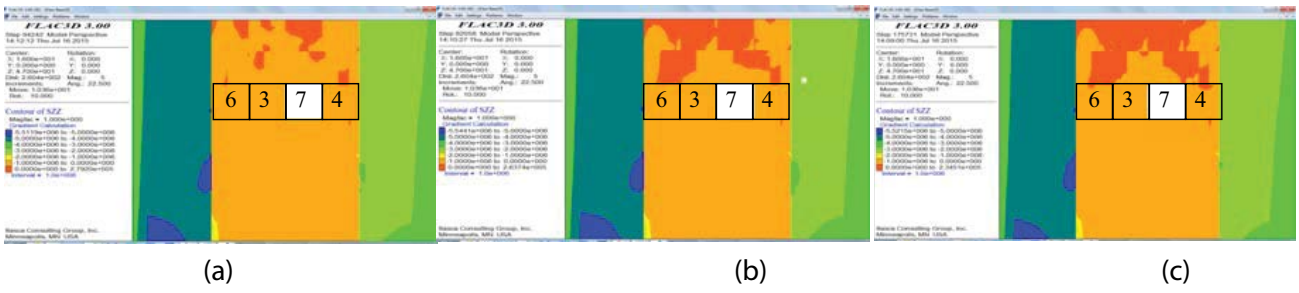

Fig. 5. Vertical stress contour of false roof with different strength levels (a) 0.5 MPa, (b) 1.5 MPa, and (c) 3 MPa.

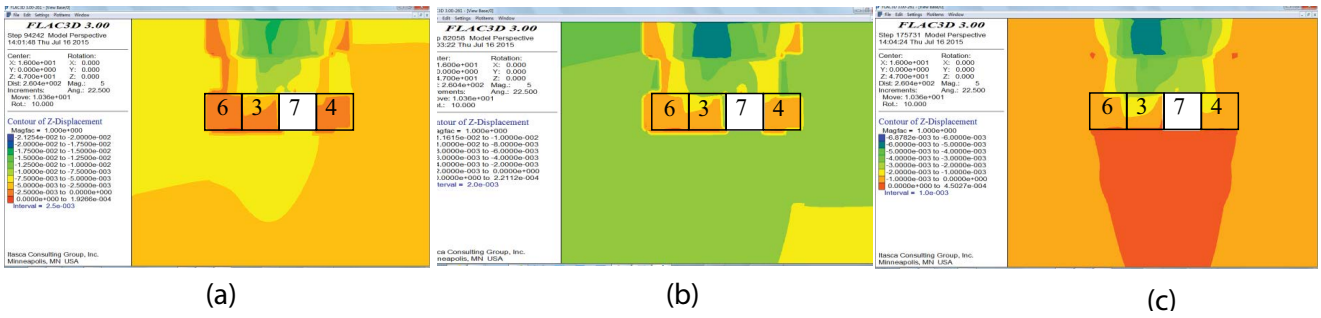

Fig. 6. Displacement contour of false roof with different strength levels (a) 0.5 MPa, (b) 1.5 MPa, and (c) 3 MPa.

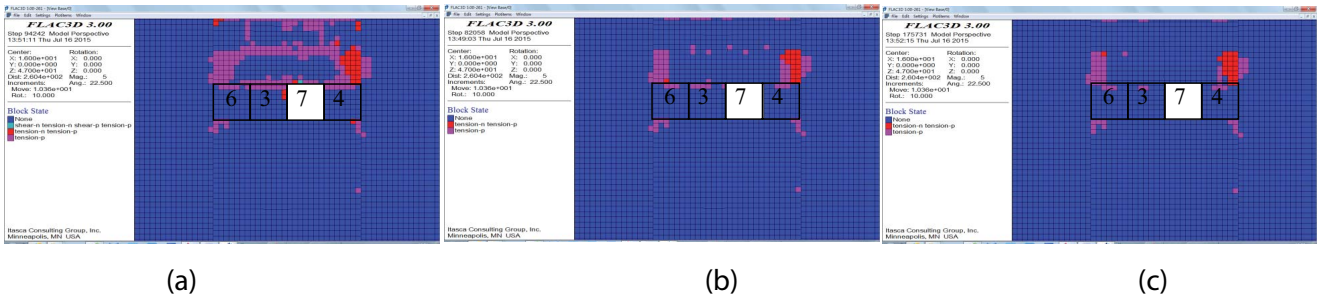

Fig. 7. Plastic zone distribution of false roof with different strength levels (a) 0.5 MPa, (b) 1.5 MPa, and (c) 3 MPa.

The breaking failure is the main failure mode of the false roof in highwall mining method. The strength of CPB plays an indispensable role in the process of ensuring stability of false roof. Controlling the CPB strength higher than 1.17 MPa is the key to prevent the broken roof from breaking and instability.

According to the numerical simulation analysis, the vertical stress on the false roof decreased to 1/3 of the original and stress concentration reduced greatly, it is conducive to maintaining the integrity of the CPB. Meanwhile, the roof subsidence reduces by about 1/3 and it provides a safer guarantee for the maintenance of roadway filling mining. When the strength is increased to 3 MPa, the range of the stress and the plastic zone of the roof are greatly reduced, and the CPB strength influence on the stability of the false roof is negligible.

It will be the most reasonable for the strength control of CPB to adjust 0.08 mm gangue content to be 25% instead of the bigger the better. Compared with the effect of mass concentration and cement content, it is more favorable for cost reduction of mining to control the cement content and increase the mass concentration.

Acknowledgments

The present research work was supported by the National key basic research development program subproject (973 Program: 2015CB25160); A Project Funded by the Priority Academic Program Development of Jiangsu Higher Education Institutions (PAPD); the Fundamental Research Funds for the Central Universities (NO. 2014XT01); the Special Funds of Taishan Scholar Construction Project of China (201309); the National Natural Science Foundation of China (Grant No. 52074270).

References

[1] X. Dong, A. Karrech, H. Basarir, M. Elchalakani, A. Seibi, Energy dissipation and storage in underground mining operations, Rock Mech. Rock Eng., 52 (2019) 229–245.
[2] Q. Sun, J. Zhang, N. Zhou, Study and discussion of short-strip coal pillar recovery with cemented paste backfill, Int. J. Rock Mech. Min. Sci., 104 (2018) 147–155.
[3] J. Zhang, Q. Sun, A. Fourie, F. Ju, X. Dong, Risk assessment and prevention of surface subsidence in deep multiple coal seam mining under dense above-ground buildings: case study, Hum. Ecol. Risk Assess., 25 (2019) 1579–1593.
[4] X. Dong, A. Karrech, H. Basarir, M. Elchalakani, C. Qi, Analytical solution of energy redistribution in rectangular openings upon in-situ rock mass alteration, Int. J. Rock Mech. Min. Sci., 106 (2018) 74–83.
[5] M. Fraldi, F. Guarracino, Analytical solutions for collapse mechanisms in tunnels with arbitrary cross sections, Int. J. Solids Struct., 47 (2010) 216–223.
[6] F. Song, H. Wang, M. Jiang, Analytical solutions for lined circular tunnels in viscoelastic rock considering various interface conditions, Appl. Math. Model., 55 (2018) 109–130.
[7] X. Dong, A. Karrech, H. Basarir, M. Elchalakani, Extended Finite Element Modelling of Fracture Propagation During In-Situ Rock Mass Alteration, 52nd US Rock Mechanics/Geomechanics Symposium, American Rock Mechanics Association, Seattle, Washington, USA, 2018, pp. 1–8.
[8] Y. Huang, J. Li, Y. Teng, X. Dong, X. Wang, G. Kong, T. Song, Numerical simulation study on macroscopic mechanical behaviors and micro-motion characteristics of gangues under triaxial compression, Powder Technol., 320 (2017) 668–684.
[9] C.A. Tang, H. Liu, P.K.K. Lee, Y. Tsui, L. Tham, Numerical studies of the influence of microstructure on rock failure in uniaxial compression—part I: effect of heterogeneity, Int. J. Rock Mech. Min. Sci., 37 (2000) 555–569.
[10] W. He, A. Hayatdavoudi, H. Shi, K. Sawant, P. Huang, A preliminary fractal interpretation of effects of grain size and grain shape on rock strength, Rock Mech. Rock Eng., 52 (2019) 1745–1765.

[11] H.G. Ji, H. Jiang, Z.Y. Song, Z.Q. Liu, J. Tan, Y.J. Liu, Y.F. Wu, Analysis on the microstructure evolution and fracture morphology during the softening process of weakly cemented sandstone, J. China Coal Soc., 43 (2018) 993–999.
[12] M.M. Islam, A.Z. Ahmed, S.F. Kabir, R. Islam, M.A.I. Molla. Optimization of photodegradation conditions of Rhodamine B in water with dye-sensitized titanium dioxide, J. Clean WAS, 4 (2020) 28–31.
[13] Y.L. Chen, Q.X. Cai, T. Shang, Z.X. Che, Mining system for remaining coal of final highwall, J. Min. Sci., 47 (2011) 771–777.
[14] Y. Chen, H. Shimada, T. Sasaoka, A. Hamanaka, K. Matsui, Research on exploiting residual coal around final end-walls by highwall mining system in China, Int. J. Min. Reclam. Environ., 27 (2013) 166–179.
[15] W.G. Liu, L.S. Wang, Q. Fu, SHM high-wall mining technology and key issues of application, Coal Eng., 6 (2012) 002.
[16] B. Prabal, H.R. Syed, Resilience of agriculture farmers for crop production in responses to climate change impact on South-Eastern Coast of Bangladesh, Environ. Ecosyst. Sci., 4 (2020) 28–37.
[17] C.Y. Liu, J.X. Yang, F.F. Wu, A proposed method of coal pillar design, goaf filling, and grouting of steeply inclined coal seams under water-filled strata, Mine Water Environ., 34 (2015) 87–94.
[18] Z.Q. Luo, C.Y. Xie, N. Jia, B. Yang, G.H. Cheng, Safe roof thickness and span of stope under complex filling body, J. Cent. South Univ., 20 (2013) 3641–3647.
[19] H.L. Venegas- Quiñones, M. Thomasson, P.A. Garcia-Chevesich, Water scarcity or drought? The cause and solution for the lack of water in Laguna De Aculeo, Water Conserv. Manage., 4 (2020) 42–45.
[20] Q.L. Chang, H.Q. Zhou, J.B. Bai, Stability study and practice of overlying strata with paste backfilling, J. Min. Saf. Eng., 28 (2011) 279–282.
[21] Q.F. Chen, K.P. Zhou, L.L. Wang, Stress field evolution law of mining environment reconstructing structure with change of filling height, J. Cent. South Univ., 17 (2010) 738–743.
[22] X.Z. Hua, H.H. Sun, Study on main parameters of underhand heading filling with high-water content tailings, J. China Univ. Min. Technol. (in Chinese), 30 (2001) 99–102.
[23] X. Peng, X.B. Li, Q.L. Zhang, X.M. Wang, Quality evaluation of layer like backfilling and flow pattern of backfill slurry in stope, J. Cent. South Univ., 14 (2007) 580–583.
[24] J. Zhang, Q. Sun, N. Zhou, J. Haiqiang, D. Germain, S. Abro, Research and application of roadway backfill coal mining technology in western coal mining area, Arab. J. Geosci., 9 (2016) 558.
[25] C.Z. Zhao, H.Q. Zhou, Q.D. Qu, M.L. Guan, Preliminary test on mechanical properties of paste filling material, J. China Univ. Min. Technol., 33 (2004) 159–161.